DTU Library

PIV measurements of flow structures in a spray dryer

Meyer, Knud Erik; Velte, Clara Marika; Ullum, Thorvald

PIV measurements of flow structures in a spray dryer

Knud Erik Meyer[1], Clara M. Velte[1] and Thorvald Ullum[2]

[1]Department of Mechanical Engineering, Technical University of Denmark, Lyngby, Denmark
kem@mek.dtu.dk

[2]GEA Niro, Søborg, Denmark
thorvald.ullum@geagroup.com

ABSTRACT

Stereoscopic Particle Image Velocimetry (PIV) measurements are made in horizontal planes in a simplified scale model of a spray dryer using water as fluid. The sample rate was sufficient to resolve phenomena at lower frequencies. Data reveal asymmetric velocity fields in both mean fields and dynamics. Data were analysed using Proper Orthogonal Decomposition (POD). An important periodic event is an elongation of the jet core cross section that results in a downstream displacement of the jet towards the chamber wall.

1. INTRODUCTION

A spray dryer typically consists of a cylindrical chamber where hot air enters at the top along the centre line as a swirling or non-swirling jet. The liquid to be dried is then atomized into this jet. The dried material settles at the bottom while the air leaves the chamber through one or more outlets on the chamber walls. The flow in the chamber has high turbulence intensity, but it also contains large-scale flow structures that appears at low frequencies. The flow is therefore challenging to model by Computational Fluid Dynamics (CFD). The purpose of this paper is to study the general flow phenomena, in particular flow structures and events. We also aim to provide data that can be used for validation of CFD simulations.

Free and confined swirling jets have been studied for several decades. An example is a recent study by Martinelli *et al* [1] that used Particle Image Velocimetry (PIV) and Laser Doppler Velocimetry (LDV) to characterise the precessing vortex core. Only few studies of detailed velocity measurements in spray dryers have been reported in the literature. Most studies have used point measurements of velocities and qualitative visualisations. Examples are the studies by Southwell and Langrish. They used several visualisation techniques [2] and LDV [3]. They found that the flow was characterised by very high RMS values and non-axisymmetric large-scale flow patterns. Lebarbier *et al* [4] used image analysis of visualisation videos to extract information about frequencies in the flow, e.g., for the jet precession.

The present study uses a scale model of a spray dryer with water as the fluid instead of air, with isothermal conditions and with no liquid atomized in the jet. The cylindrical chamber has a single outlet in the side.

2. SETUP AND MEASUREMENT PROCEDURE

A sketch of the experimental setup is shown in figure 1. Tap water is used at the fluid. The water flow is created with a frequency controlled pump, and the flow rate is measured with an electro-magnetic flow meter. The chamber has sides made of transparent polycarbonate. The chamber consists of a
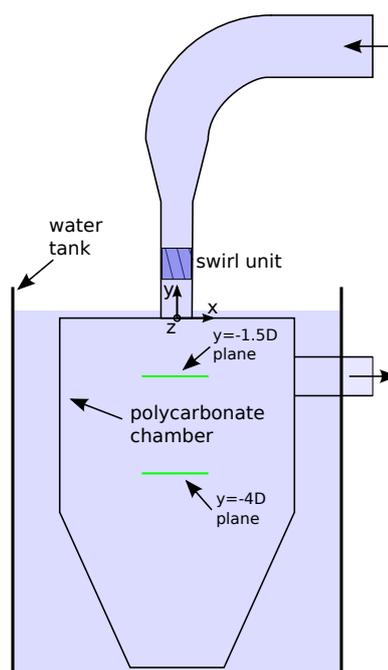

Figure 1: Experimental setup.

cylindrical part with inner diameter of 290 mm and a height of 250 mm and below that a conical part that reduces the diameter from 290 mm to 124 mm over a height of 200 mm. Top and bottom are covered with plates. The inlet is a pipe with an inner diameter of $D = 50.5$ mm mounted at the centre of the top plate. A distance D upstream into the inlet pipe, a swirl unit is placed. The swirl unit consists of 6 plates that are connected to a centred cylindrical rod with a diameter of 6 mm. The plates have an angle of $8°$ with respect to axial direction. The height of the swirl unit is D. One D above the swirl unit, a conical section connects to a pipe with inner diameter of 75 mm. This immediately connects to a $90°$ pipe bend with an inner radius also of 75 mm. A 650 mm long piece of pipe then connects to a new pipe bend and then to a long pipe that connects to the pump. The pump recirculates water from the outlet. The outlet is a rectangular duct with height D and width $2D$, and it is placed at the side of the cylindrical part of the chamber. The top of the outlet is one D below the top plate.

The coordinate system is shown in figure 1. It has origin in the centre of the inlet. The x-direction is towards the outlet and the y-direction goes along the axis of the inlet pipe pointing into the inlet pipe. The z-direction follows by the definition of a right-handed coordinate system. Velocity vector components follow the coordinate directions (x, y, z) and is denoted (u, v, w). We use uppercase letters to denoted components of the mean
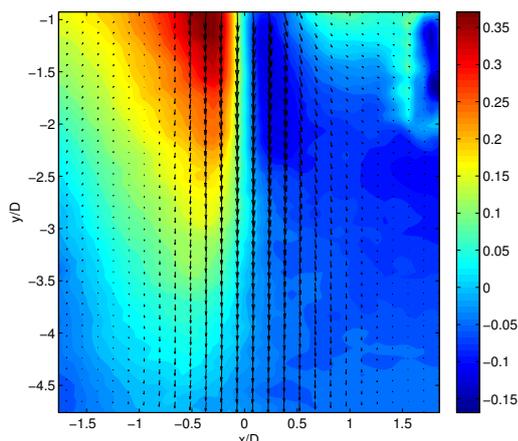
Figure 2: Mean velocity field at the $z = 0$ plane (from [6]), color contours indicate W/U_{in}

velocity (U, W, V).

The spray dryer chamber is placed in a larger water-filled tank with 8 vertical glass windows. The measurements are done with a Particle Image Velocimetry (PIV) system that consists of a 200 mJ Nd:YAG laser and two Dantec Hisense mk II cameras with Scheimpflug mounts allowing stereoscopic PIV measurements. Cameras each have a 35 mm focal length lens and uses an aperture of $F_{\#} = 8$. Cameras are fitted with narrow band filters at the laser light wavelength of 532 nm. Silver-coated hollow glass spheres with a diameter of 10 μm are added to the water as seeding. Water-filled prisms are glued on to the tank windows to accommodate stereoscopic measurements in horizontal planes. The prisms windows have an angle of $45°$ with the y-axis and are parallel with x axis.

Measurements are made with an bulk mean velocity at the inlet pipe of $U_{\text{in}} = 4.0$ m/s. The water temperature is $20.5\pm0.5°$C. The flow corresponds to a Reynolds number based on inlet mean velocity and inlet diameter of Re $= U_{\text{in}}D/\nu = 201000$. Measurements are done with a sample rate of 4 Hz. Two horizontal planes are investigated: $y = -1.5D$ and $y = -4D$. The position $y = -1.5D$ corresponds to the mid-point of the outlet. The position $y = -4D$ is further downstream in the jet, but still one D above the start of the conical part of the chamber. The measurement region spans $1.5D$ in the x-direction and $2.5D$ in the z-direction. This region was limited by different geometrical constraints and it covers the jet from the inlet, but not flow closer to the walls. For each plane, five series of 512 samples where taken giving a total of 2560 samples.

3. POD ANALYSIS

We use the same type of snapshot Proper Orthogonal Decomposition (POD) analysis as described by Meyer *et al* [5]. POD analysis finds "modes" that decompose a snapshots fluctuations from the mean fields in an "optimal" way using eigenvectors of the cross correlation between snapshots. The eigenvalue represents the part of the kinetic energy of fluctuations from the mean field that a particular mode accounts for. A snapshots can be reconstructed perfectly by multiplying each mode i with a corresponding reconstruction coefficient a_i and adding the sum of these products to the mean field. Modes are sorted with respect to energy with the most energetic mode as mode 1. A particular snapshot can therefore often be reconstructed satisfactorily using a few of the first modes.
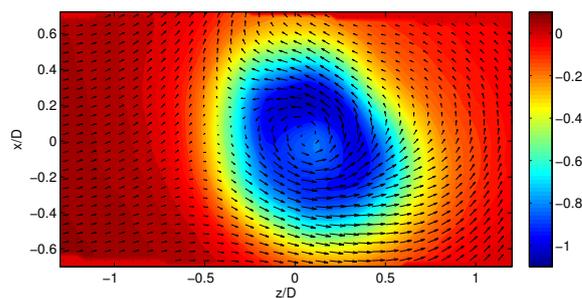

Figure 3: Mean velocity field at the $y = -1.5D$ plane, color contours show V/U_{in}.

4. RESULTS

We will mainly present results as vector fields of velocities or POD modes. Plots of fields only show every second vector in each direction for visual clarity. The out-of-plane component is shown as color contours. The region with data is not completely rectangular due to the optical arrangement. Some regions in our rectangular plots are therefore filled with vector of zero length near the sides. A first set of measurements were made by Jensen and Hansen [6] in the vertical plane $z = 0$. Their measurement of the mean flow field was based on 1900 snapshots and is shown in figure 2. The jet flow is in the negative y-direction. There is a strong swirl near the inlet, but the swirl decreases significantly in downwards direction. The swirl-component is stronger for negative x than for positive x. The reason is that the outlet is located in the positive x-direction. The region with low velocities in the upper-right corner of the plot is an artifact caused by reflections from the outlet.

Figure 3 shows the mean velocity field at the $y = -1.5D$ plane. The outlet is at $x = 2.9D$ and therefore at some distance from the plotted region, but its presence is clearly seen in the velocity field since all velocity vectors along $x = 0.6D$ have a positive U velocity component. The shape of the jet indicated as the region with large negative values of V (blue color) is somewhat asymmetrical with more of the jet going through the quadrant with $x < 0$ and $z > 0$ than the other three quadrants. There is a small wake in the centre of the jet with smaller magnitude of V. This could be a wake effect of the rod in the middle of the swirl generator, but could also be related to the swirl distribution itself.
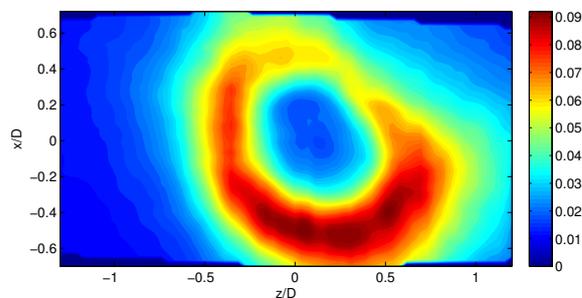

Figure 4: Turbulent kinetic energy k/U_{in}^2 at the $y = -1.5D$ plane.

Figure 4 show the turbulent kinetic energy k in the same plane. High levels of k are as expected found in a ring around the jet corresponding to the region with high gradients in the V velocity component. However, the levels are much higher at negative x positions indicating that the flow dynamics also appear in a
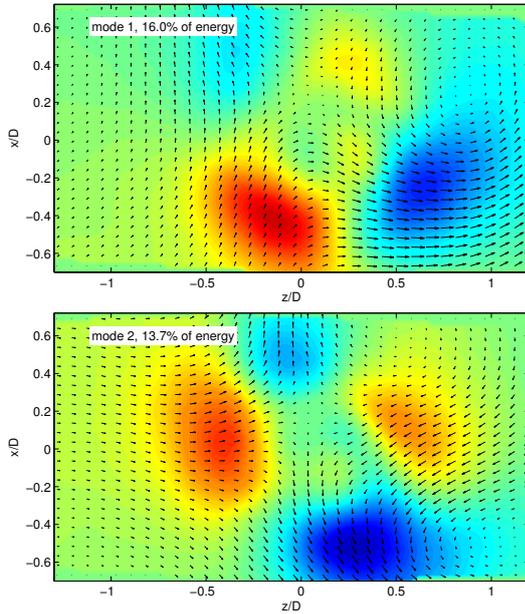
non-symmetric way.

Figure 5: The first two POD-modes at $y = -1.5D$ plane, color contours indicate out-of-plane component.

The two first POD modes in the $y = -1.5D$ plane are shown in figure 5. These two modes together represent 30% of the energy of velocity fluctuations. The next mode (mode 3) represents only 6% of the energy and thus significantly less. Mode 1 and 2 both have two regions of high positive and high negative out-of-plane component arranged in a circular pattern at positions corresponding to the edge of the jet. Adding mode 1 multiplied by a positive coefficient a_1 to the mean field results in a more elliptical shaped jet core with a main axis that has an angle of about $45°$ with the x and z axes. Adding mode 2 multiplied by a negative coefficient a_2 will give an elliptical shaped jet core with main axis in the z-direction. A combination of the two modes can give any angle of such a elliptical shape of the jet.

The variation of the reconstruction coefficient a_1 and a_2 for the first 512 snapshots is shown in figure 6(top). The plot shows periodic variations in the coefficient with a period of a bit less than 10 seconds. For a_1, peaks of positive values have large numerical value than peaks with negative values. The opposite is true for a_2. A repeating event seems to be that a large negative peak in a_2 is followed by a large positive peak in a_1. An example of snapshots from such an event is also shown in figure 6. At time $t = 68.5$ s, both a_1 and a_2 have relatively low numerical values. The snapshot is quite symmetrical. At $t = 69.0$ s, we have a large negative values of a_2, moderate value of a_1 and the jet core has is strongly elongated in the z-direction. At $t = 71.0$ s, we have a large positive value of a_1, moderate value of a_2 and the elongated jet core has now turned $45°$. FFT analysis of the time signal for the full data series for both a_1 and a_2 is shown in figure 7. The FFT analysis uses block averaging of the five data series with each 512 samples. The frequency spectrum has a clear peak at 0.12 Hz for both coefficients. An earlier measurement on a slightly smaller region gave very similar POD modes and a dominating frequency of 0.14 Hz.

The mean velocity field at the $y = -4D$ plane is shown in figure 8 together with the two first POD modes. The mean field has the same type of asymmetry as observed for the $y = -1.5D$

plane, but the jet core has expanded in size. The two first POD modes together represents 20% of the energy of the velocity fluctuations. This is lower than for the $y = -1.5D$ plane and this indicates that fluctuations are more complex. POD modes 1 and 2 now both have a single region with positive out-of-plane component and a single region with negative out-of-plane component. Adding mode 1 or mode 2 to the mean field acts to displace the position of the jet core.
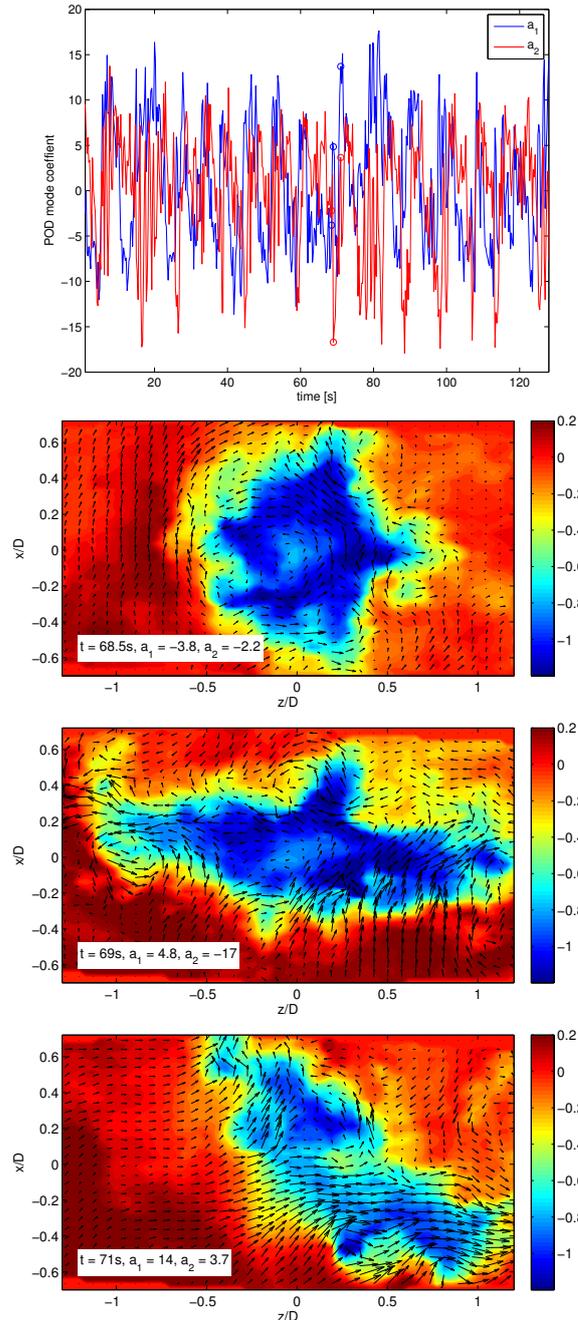

Figure 6: Time history of POD reconstruction coefficients (top) and selected snapshots at $y = -1.5D$, color contours show V/U_{in}.

Figure 9 show the time history of a_1 and a_2 for the first 512 samples measured in the $y = -4D$ plane. The variation is less regular than for the $y = -1.5D$ plane, but systematically appearing peaks can still be observed for the two reconstruction coefficients. A FFT analysis of all 2560 samples finds a clear
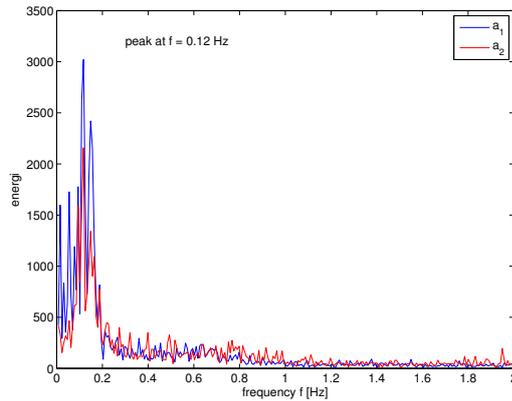
Figure 7: Frequency spectrum for the two first POD reconstruction coefficients from the $y = -1.5D$ plane

peak at 0.14 Hz for both a_1 and a_2. Figure 9 also shows a snapshot for the highest value of a_1 found in the time history (at $t = 1.5$ s). The jet region is clearly displaced towards positive value of both x and z.

The POD analysis is also done on two more case. The first case uses data from [6] for the $z = 0$ plane. Figure 10 show the first POD mode. The out-of-plane component is small compared to higher modes and is therefore shown with only small changes in colors. The main variation from this modes is therefore in the y-direction. This mode is in reasonable agreement with mode 2 from the $y = -1.5D$ plane and mode 1 from the $y = -4D$ plane. An FFT analysis of the reconstruction coefficients shows a broader range of frequencies with high energy, but it finds the highest peak at a frequency of 0.13 Hz and an a peak with almost the same height at twice that frequency. This is in good agreement with measurements in horizontal planes. The following POD modes have significantly less clear peaks in the frequency spectrum. The second case is a series in the $y = -1.5D$ plane with inlet velocity $U_{in} = 3.0$ m/s. The POD modes are almost identical to measurements with $U_{in} = 4.0$ m/s and the FFT analysis finds a frequency of 0.086 Hz.

5. DISCUSSION OF FREQUENCIES

Earlier studies have also identify low-frequency flow phenomena in spray-dryers. An example is [4] that uses a Strouhal number defined as $St = (2/\sqrt{\pi})E^2 fD/U_{in}$, where E is the ratio between chamber diameter and inlet diameter and f is the frequency. The lowest observed frequencies in [4] has $St = 0.04$ for no swirl and $St = 0.08$ for a case with $25°$ swirl vane angle. Data are based in image analysis of video visualisation and are attributed to a precession of the central jet. Our measured frequencies give $St \approx 0.062$ for the $U_{in} = 4$ m/s and $St = 0.055$ for the $U_{in} = 3$ m/s. The frequencies are therefore similar to the ones found by [4].

6. CONCLUSIONS

Measurements show that the flow in a model of spray dryer has large fluctuations and that a major contribution to the fluctuations is a flow event appearing at low frequency. Near the jet exit, the jet core cross section quite suddenly gets elongated and this shape rotates less than $180°$ before the shape get more circular again for a longer period. Further downstream in the cylinder, the event shows up as a displacement of the jet core position in a preferred direction. Due to the asymmetry in this event, it should probably not be characterised as jet precession,

but a jet instability that couples to the rest of the flow in the chamber.

This kind of flow events are difficult to detect because it is going on together with strong turbulent fluctuations. A set of LDV measurement did not detect a clear frequency in FFT analysis. The use of POD on PIV data proved to be a very useful tool.

ACKNOWLEDGMENTS

REFERENCES

[1] Martinelli, F., Olivani, A. & Coghe, A. (2007) Experimental analysis of the precessing vortex core in a free swirling jet. *Experiments in Fluids*, **42**, 827–839.

[2] Southwell, D.B. & Langrish, T.A.G. (2000) Observations of flow patterns in a spray dryer. *Drying technology*, **18**, 661–585.

[3] Southwell, D.B. & Langrish, T.A.G. (2001) The effect of swirl on flow stability in spray dryers. *Trans IChemE*, **79(A)**, 222–234.

[4] Lebarbier, C., Kockel, T.K., Fletcher, D.F. & Langrish, T.A.G. (2001) Experimental measurements and numerical simulation of the effect of swirl on flow stability in spray dryers. *Trans IChemE*, **79(A)**, 260–268.

[5] Meyer, K.E., Pedersen, J.M. & Özcan, O. (2007) A turbulent jet in crossflow analysed with proper orthogonal decomposition. *Journal of Fluid Mechanics*, **583**, 199–227.

[6] Jensen, B. K. & Hansen, J. E. (2011) PIV-målinger i model af spraytørrer (in Danish). *Bachelor thesis*, Department of Mechanical Engineering, Technical University of Denmark, MEK-FM-BA-2011-02.
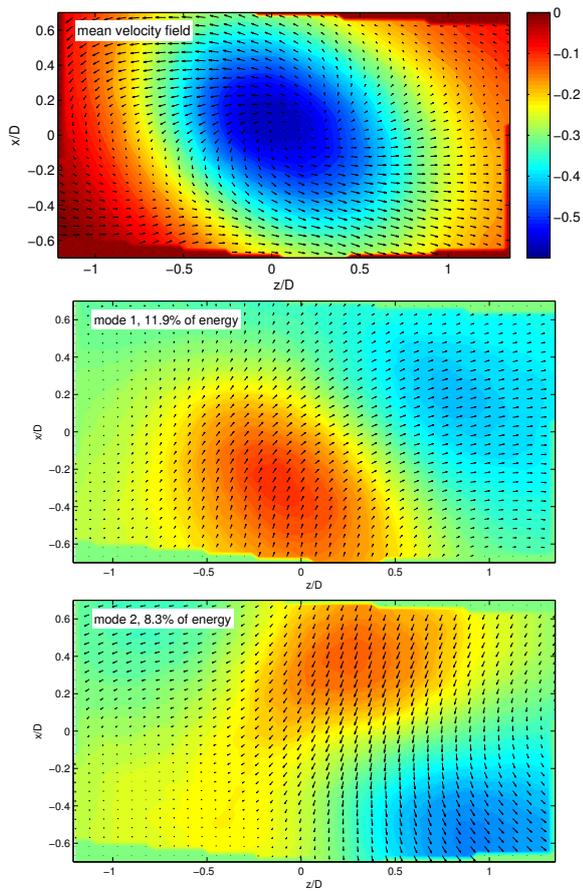
Figure 8: Mean velocity field (top) and the first two POD-modes at the $y = -4D$ plane, color contours indicate V/U_{in} or just out-of-plane component, respectively.

Figure 10: The first POD mode at the $z = 0$ plane, color contours indicate out-of-plane component.
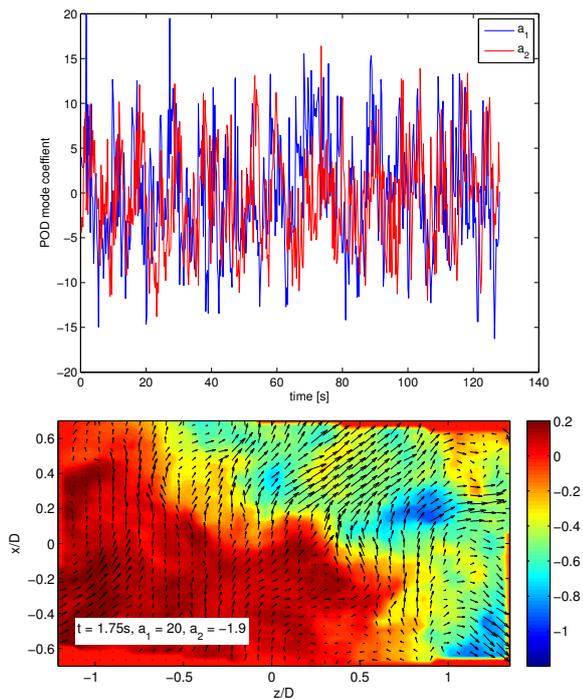

Figure 9: Time history of POD reconstruction coefficients (top) and a selected snapshots at $y = -4D$, color contour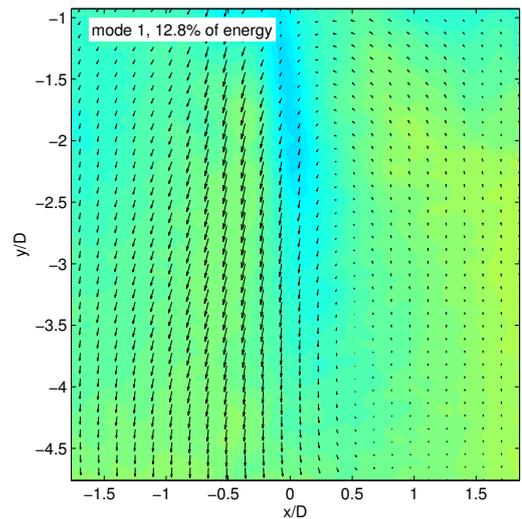s indicate out-of-plane component.